

Click Reaction Synthesis and Photophysical Studies of Dendritic Metalloporphyrins

Nguyen Tran Nguyen,^[a] Johan Hofkens,^[b] Ivan G. Scheblykin,^[c] Mikalai Kruk,^[d,e] and Wim Dehaen^{*[a]}

Keywords: Porphyrinoids / Dendrimers / Luminescence / Photochemistry / Fluorescence / Click chemistry

Several dendritic zinc(II)-porphyrins bearing carbazole units at the terminals have been prepared through click reaction of azide-substituted Zn-porphyrin precursors and carbazole-based alkynes under $[\text{Cu}(\text{NCCCH}_3)_4][\text{PF}_6]$ catalysis. This family of new dendritic metalloporphyrins shows dual luminescence from both the upper S_2 and the lowest S_1 singlet states. The observed trends in the spectroscopic data and the photophysical properties of the dendrimers have been rationalized in terms of the type of *meso*-spacer between the macrocycle and dendritic shell. The key feature of the *meso*-spacer is proposed to be the degree of hindrance towards aryl ring rotation relative to the mean porphyrin plane. Based on the observed differences in the $S_1 \rightarrow S_0$ fluorescence quantum

yield on going from four- to five-coordinate dendrimers, it was shown that dendrimer architectures with all four *meso*-aryl spacers sterically hindered, are most appropriate to monitor processes related to axial ligation of the dendrimer core, since they provide larger luminescence response differences between the four-coordinate and five-coordinate forms. The blue $S_2 \rightarrow S_0$ fluorescence quantum yield has been measured and the observed trend has been rationalized in terms of the $S_2 \rightarrow S_1$ energy gap law. No significant differences were observed between the compounds either with different rotational degree of freedom of the *meso*-spacers or with different ligation states of the dendrimer core.

Introduction

Porphyrin-based materials have been receiving considerable attention due to their numerous applications, with the most important of them being in material chemistry,^[1] catalytic chemistry,^[2] sensor design,^[3] photodynamic therapy,^[4] and organic photovoltaics.^[5] Dendritic encapsulation brings to the core molecule new features and allows several of their own properties to be either enhanced or suppressed.^[6] Therefore, the design of new dendritic porphyrins (which can also be named as dendrimers with a porphyrin core) with particular structure and properties is of considerable interest,^[7] and substantially extends the potential of porphyrin applications. The choice of the dendron type is cru-

cial for the structure and functional properties of designed dendrimer molecules. Carbazole derivatives can be considered as promising dendron molecules that could be used to prepare new functional dendrimers with a porphyrin core.^[8] Carbazole is an electron-rich conjugated system in which the 3-, 6-, and 9-positions are the most reactive sites towards electrophilic substitution.^[9] Aryl substituents at the 9-position of the carbazole will result in a decrease in energy of the HOMO level^[10] and so carbazole derivatives can be used as host material in light-emitting devices.^[11] Different approaches have been used to achieve high generation dendrimers,^[7] with click chemistry (more specifically the click reaction) being suggested as a reliable and useful tool with which to achieve this goal. Thus, copper(I)-catalyzed 1,3-dipolar cycloaddition of azides and terminal alkynes is regioselective for the formation of 1,4-disubstituted 1,2,3-triazole products in high yields.^[12] The 1,2,3-triazole group has been considered a significantly π -conjugated linker in intramolecular energy transfer (ET) processes.^[13] In the field of porphyrin chemistry, a series of triazole-linked zinc(II)porphyrin-fullerenes was synthesized and their photophysical properties were also reported.^[13b,14] Heterometallic, multiporphyrin dendrimers made by click chemistry have shown rather efficient energy- and electron-transfer reactions that can be used for solar energy conversion.^[15] The coordination of the nitrogen atoms of the triazole rings to the Zn ions of the porphyrins, together with π - π interactions between the zinc porphyrins bring about

[a] Molecular Design and Synthesis, Department of Chemistry, KU Leuven,

Celestijnenlaan 200F, 3001 Leuven, Belgium
E-mail: wim.dehaen@chem.kuleuven.be
<http://chem.kuleuven.be/en/research/mds/losa>

[b] Molecular Imaging and Photonics, Department of Chemistry, KU Leuven,

Celestijnenlaan 200F, 3001 Leuven, Belgium

[c] Lund University, Department of Chemical Physics,
P. O. Box 124, 22100 Lund, Sweden

[d] Belarussian State Technological University, Physics
Department,

Sverdlova str. 13a, 220050 Minsk, Belarus

[e] B. I. Stepanov Institute of Physics of National Academy of
Sciences,

Pr. Nezavisimosti 68, 220072 Minsk, Belarus

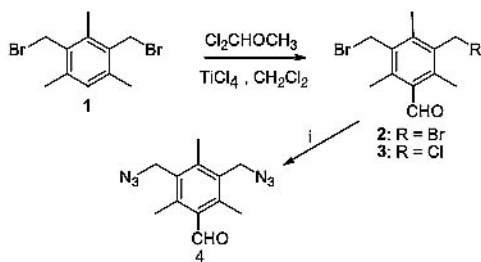
Supporting information for this article is available on the
WWW under <http://dx.doi.org/10.1002/ejoc.201301158>.

dramatic changes in the conformation and photophysical properties.^[13a,13c,16] A smart porphyrin cage that was made by click chemistry showed novel binding ability toward azide anions.^[17] To the best of our knowledge, there have been no reports on the linkage of porphyrin and carbazole derivatives through application of the click reaction. In this paper, we report on the synthesis of a family of new dendritic porphyrins through the click reaction starting from azido porphyrins and carbazole-based alkynes under $[\text{Cu}(\text{NCCCH}_3)_4][\text{PF}_6]$ catalysis, and discuss the photophysical properties of the target dendrimers.

Results and Discussion

Synthesis

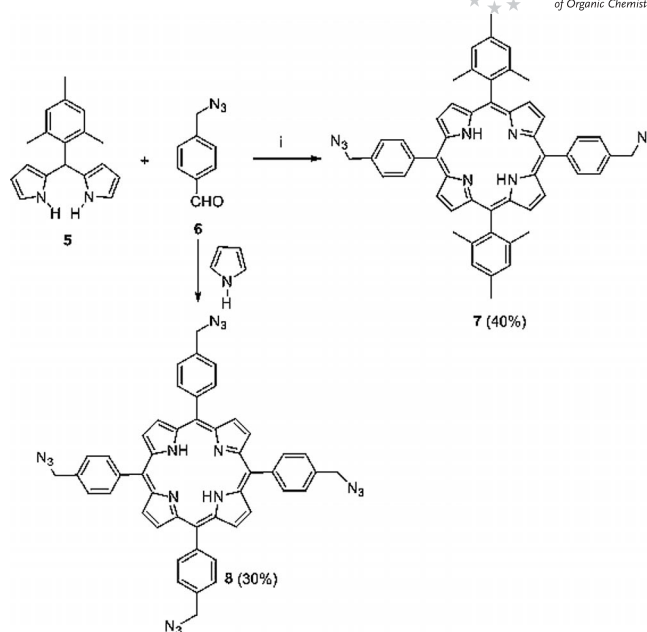
The synthesis of 3,5-bis(azidomethyl)-2,4,6-trimethylbenzaldehyde (**4**) was based on the synthesis of mesitaldehyde by treatment of aromatic compounds with dichloromethyl methyl ether in the presence of a Lewis acid such as TiCl_4 .^[18] However, reaction of the known 1,3-bis(bromomethyl)-2,4,6-trimethylbenzene (**1**)^[19] and dichloromethyl methyl ether resulted in the formation of not only 3,5-bis(bromomethyl)-2,4,6-trimethylbenzaldehyde (**2**) but also 3-bromomethyl-5-chloromethyl-2,4,6-trimethylbenzaldehyde (**3**), according to mass and ^1H NMR spectroscopy analyses. When purification by column chromatography was carried out, these two aldehydes could not be obtained in pure form. Therefore, this mixture of arylaldehydes was treated with sodium azide to give 3,5-bis(azidomethyl)-2,4,6-trimethylbenzaldehyde (**4**) in pure form (Scheme 1).



Scheme 1. Reagents and conditions: (i) NaN_3 , $\text{CH}_3\text{COCH}_3/\text{H}_2\text{O}$ (4:1), reflux, overnight.

The synthesis of 5,15-bis(2,4,6-trimethylphenyl)-10,20-bis(4-azidomethylphenyl) porphyrin (**7**) was based on the Lindsey method starting from 5-mesityldipyromethane (**5**)^[20] and 4-(azidomethyl)benzaldehyde (**6**).^[21] Porphyrin 5,10,15,20-tetrakis(4-azidomethylphenyl)porphyrin (**8**),^[17] was prepared from 4-(azidomethyl)benzaldehyde (**6**)^[21] and pyrrole (Scheme 2).

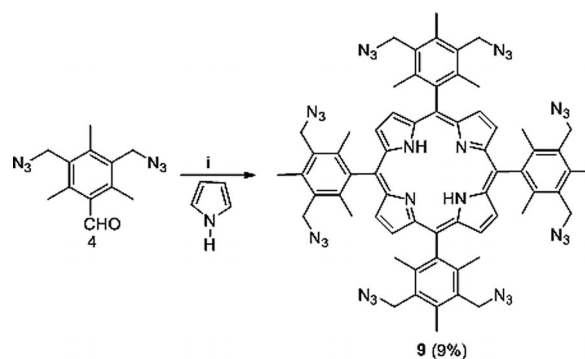
With a concentration of starting materials of 10 mM in anhydrous CH_2Cl_2 , the yield of **7** reached 40% with 0.3 equiv. $\text{BF}_3\cdot\text{OEt}_2$ (see the Supporting Information, Table S1). When the conditions optimized for the synthesis of **7** were applied to make 5,10,15,20-tetrakis(3,5-bis(azidomethyl)-2,4,6-trimethylphenyl)porphyrin (**9**), no target compound was obtained. In further attempts to prepare the desired compound **9**, trifluoroacetic acid (TFA) was also tried



Scheme 2. Reagents and conditions: (i) 1. $\text{BF}_3\cdot\text{OEt}_2$ (0.3 equiv.), CH_2Cl_2 , room temp., 1 h; 2. *p*-chloranil, reflux, 1 h.

as catalyst for the condensation between **4** and pyrrole, but no porphyrin was obtained. Similarly, the reaction of mesitaldehyde and pyrrole in CH_2Cl_2 with either $\text{BF}_3\cdot\text{OEt}_2$ or TFA catalyst afforded no porphyrin. However, tetramesityl porphyrin was obtained in 29–32% yield in the presence of 0.75% absolute ethanol in anhydrous CH_2Cl_2 .^[22]

With 0.3 equiv. $\text{BF}_3\cdot\text{OEt}_2$ and 10 mM concentration of reactants, the synthesis of **9** in anhydrous CH_2Cl_2 containing 0.75% absolute ethanol was unsuccessful, and no porphyrin appeared. Finally, when the amount of catalyst was increased to 0.8 equiv., porphyrin **9** was obtained in a low but reasonable yield of 9% (Scheme 3).

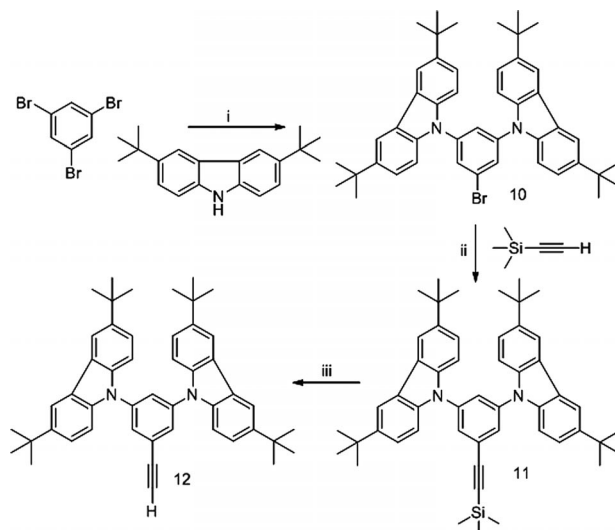


Scheme 3. Reagents and conditions: (i) 1. $\text{BF}_3\cdot\text{OEt}_2$ (0.8 equiv.), absolute $\text{C}_2\text{H}_5\text{OH}$ in CH_2Cl_2 (0.75%), room temp., 1 h; 2. *p*-chloranil, reflux, 1 h.

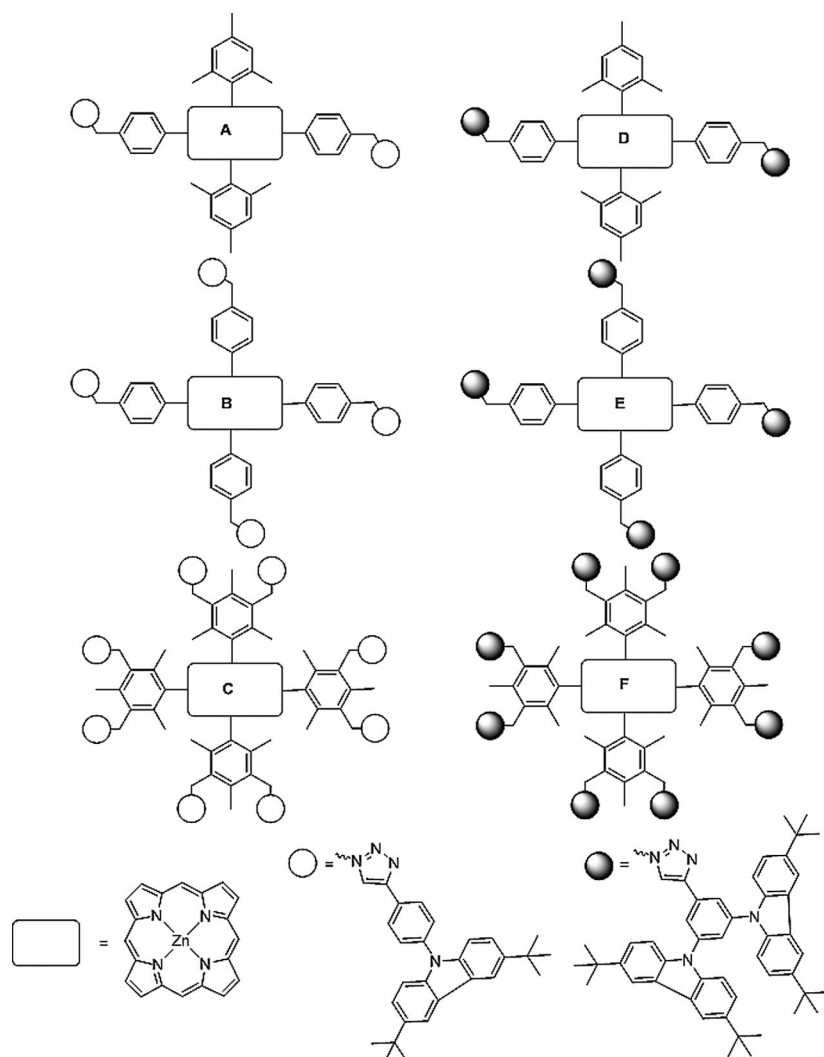
In the Ullmann coupling, the rate-determining step is the loss of halide from the aryl halide stage, and the order of reactivity of aryl halides is well-known ($\text{Ar-I} > \text{Ar-Br} > \text{Ar-Cl} \gg \text{Ar-F}$).^[23] Based on the Ullmann N-arylation of carbazoles and aryl halides, a low yielding (27%) synthesis of 1-bromo-3,5-bis[3,6-bis(*tert*-butyl)carbazol-9-yl]benzene

(**10**) by condensation of 1,3,5-tribromobenzene and 3,6-di-*tert*-butyl-9*H*-carbazole was reported.^[24] Goodbrand and Hu demonstrated that the addition of 1,10-phenanthroline as the copper-binding ligand accelerated the traditional Ullmann condensation catalyzed by Cu^I.^[23b] Furthermore, the reaction of aryl bromides and carbazole in the presence of 1,10-phenanthroline was also reported in good yields, ranging from 42 to 52%.^[11b,11c] Thus, the yield of **10** increased from 27 to 40% when 1,10-phenanthroline was added to the reaction mixture and *N,N*-dimethylformamide (DMF) was used as solvent. The Sonogashira reaction was then carried out under catalysis of CuI and [PPh₃]₂PdCl₂ between **10** and trimethylsilylacetylene to protected 3,5-biscarbazole phenylacetylene (**11**). Compound **11** was then deprotected to give 1-ethynyl-3,5-bis[3,6-bis(*tert*-butyl)carbazol-9-yl]benzene (**12**) in good yield (Scheme 4).

The copper(I)-catalyzed azide-alkyne cycloaddition (CuAAC reaction or click reaction) is considered a very reliable reaction that can be carried out in a variety of solvents, with various sources of Cu^I catalyst.^[12a,15c,25] To establish a suitable procedure for the synthesis of dendrimers



Scheme 4. Reagents and conditions: (i) CuI, 1,10-phenanthroline, K₂CO₃, DMF, 160 °C, overnight; (ii) [P(Ph)₃]₂PdCl₂, CuI, THF, Et₃N, 65 °C, overnight; (iii) K₂CO₃, CH₂Cl₂, CH₃OH, room temp., overnight.



Scheme 5. Synthesis of dendrimers A–F. Reagents and conditions: terminal alkyne (4–16 equiv.), [Cu(NCCH₃)₄][PF₆] (0.2–0.8 equiv.), Et₃N (2 drops), THF, 60 °C, 4 h.

through click reaction, porphyrin **7** was treated with 3,6-di-*tert*-butyl-9-(4-ethynylphenyl)carbazole^[10b,26] in tetrahydrofuran (THF) under [Cu(NCCH₃)₄][PF₆] catalysis. However, these conditions led to the formation of a non-fluorescent copper(II)-porphyrin core dendrimer, according to TLC and mass spectrometric analysis. To avoid this, free-base porphyrins **7**, **8**,^[15b,17] and **9** were initially metallated to afford zinc(II)-porphyrins in quantitative yield, then the click reaction was conducted to generate dendrimers **A–F** in good yield. There was no observable Zn/Cu exchange under the reaction conditions. Dendrimers **A–C** were obtained from the reaction of zinc(II)-porphyrin (**7**), zinc(II)-porphyrin (**8**),^[17] and zinc(II)-porphyrin (**9**), respectively, with 3,6-di-*tert*-butyl-9-(4-ethynylphenyl)carbazole.^[10b,26] Similarly, dendrimers **D–F** were obtained from the reaction of zinc(II)-porphyrins and 1-ethynyl-3,5-bis[3,6-bis(*tert*-butyl)carbazol-9-yl]benzene (**12**). To avoid side-product formation, zinc(II)-porphyrins were treated with a large excess of terminal alkynes so that all azido groups were transformed into the 1,2,3-triazole linker. Dendrimers **A**, **B**, **D** and **E** were isolated in acceptable yield (90%), whereas dendrimers **C** and **F** were obtained in yields of 30 and 26%, respectively, due to difficulties during chromatographic purification (Scheme 5).

The formation of target dendrimers was evidenced by mass spectrometry (MALDI-TOF) and NMR spectroscopy. ¹H NMR spectra clearly show that the initial signals corresponding to the α -methylene protons of the azido groups of the azido porphyrins at 4.7 ppm disappeared completely and a new methylene peak developed at 5.8 ppm that was diagnostic for the formation of triazole groups (see the Supporting Information). Gel permeation chromatography (GPC) showed that the dendrimers obtained were pure and monodisperse [polydispersity index (PDI) = 1; see the Supporting Information]. FTIR analysis indicated complete disappearance of the azide bond (2080 cm⁻¹) in dendrimers **A–F** (see the Supporting Information).

Photophysical Properties

Absorption Spectra

In the UV range, the absorption of the carbazole dendrons dominate (Figure 1). The peak position of the carbazole absorption bands remains unchanged in both the **A–C** and **D–F** series of dendrimers ($\lambda_{0,0}^{CZ} = 346.5$ and 345.0 nm, respectively). The increase in carbazole band extinction co-

efficient upon going from **D** to **E** and then to **F** dendrimer is due to an increase in the number of carbazoles attached to the porphyrin (Figure 1, inset), and essentially the same trend is also observed for the **A–C** series of dendrimers (not shown).

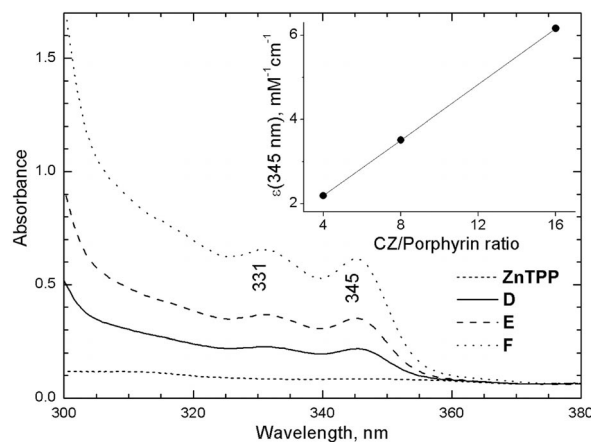


Figure 1. Absorption spectra of dendrimers **D–F** in the UV range measured for equimolar concentrations of four-coordinate Zn-porphyrin core in CH₂Cl₂. Inset shows the carbazole band extinction coefficient at 345 nm as a function of the number of attached carbazoles per porphyrin.

In the near-UV and visible ranges, the absorption profile is due to the porphyrin core. These dendrimer spectra retain all the main features of the “parent” Zn-tetra-aryl-porphyrin core (Zn-5,10,15,20-tetraphenyl-porphyrin (ZnTPP)^[27] and Zn-5,10,15,20-tetrakis(2,4,6-trimethylphenyl)-porphyrin (ZnTMesP)^[22,28]) (Tables 1 and 2). Nevertheless, minor changes could be seen in the spectra, which deserve to be discussed in detail. These subtle changes reveal the structure-property relationships of the new dendrimers and allow an understanding of how the optical properties of such dendrimers may be tuned in the desired direction. The studied dendrimers differ in the type of porphyrin core molecule, having either phenyl groups with low steric hindrance or strongly sterically hindered mesityl groups in the *meso*-positions. Two other structural differences relate to the position of the dendrons attached to the aryl ring (*para*- or *meta*-position) and the structure of the dendrons themselves. They allow the steric bulk of the dendritic shell for dendrimers **A–F** to be adjusted.

All the dendrimers have the porphyrin core chelated with Zn²⁺, thus axial ligation with oxygen- or nitrogen-containing Lewis bases is expected to take place under appropriate

Table 1. Spectral data for the studied compounds with the four-coordinate form of the Zn-porphyrin core. Solvent is CH₂Cl₂.

	$\lambda_{0,0}^{abs}$ [nm]	$\lambda_{1,0}^{abs}$ [nm]	$A_{0,0}/A_{1,0}$	$\lambda_{0,0}^{fl}$ [nm]	$\lambda_{0,1}^{fl}$ [nm]	$F_{0,0}/F_{0,1}$	$\Delta\lambda_{Stokes}$ [cm ⁻¹]
A	587.5	549.0	0.160	595.5	645.5	0.450	228
B	586.0	548.0	0.220	596.0	645.5	0.510	287
C	588.5	552.0	0.120	594.5	647.0	0.225	171
D	587.5	548.5	0.155	595.5	645.0	0.450	228
E	586.5	548.5	0.200	596.5	645.5	0.510	285
F	588.5	552.0	0.105	594.5	647.0	0.215	171
ZnTPP	585.5	547.5	0.170	595.0	645.0	0.480	272
ZnTMesP	586.0	549.0	0.090	594.0	646.5	0.240	230

Table 2. Spectral data for the studied compounds with the five-coordinate form of the Zn-porphyrin core. Solvents are THF or pyridine.

	$\lambda_{0,0}^{\text{abs}}$ [nm]	$\lambda_{1,0}^{\text{abs}}$ [nm]	$A_{0,0}/A_{1,0}$	$\lambda_{0,0}^{\text{fl}}$ [nm]	$\lambda_{0,1}^{\text{fl}}$ [nm]	$F_{0,0}/F_{0,1}$	$\Delta\lambda_{\text{Stokes}}$ [cm^{-1}]
A-THF	596.0	557.0	0.320	601.5	654.5	0.800	154
B-THF	596.0	557.0	0.400	603.0	655.0	0.900	196
C-THF	598.5	560.5	0.280	601.5	657.5	0.585	83
D-THF	596.0	557.0	0.300	601.5	654.5	0.815	154
E-THF	596.0	557.0	0.390	603.0	655.0	0.890	196
F-THF	598.5	560.5	0.285	601.5	657.5	0.600	83
F-Pyridine	605.5	567.0	0.410	610.0	666.5	0.800	122
ZnTPP-THF	594.5	555.5	0.325	600.0	653.0	0.790	154
ZnTPP-Pyridine	603.5	563.5	0.520	610.0	664.0	1.095	177
ZnTMesP-THF	595.5	558.5	0.260	598.0	654.0	0.510	71

conditions. Ligand binding studies were undertaken by us recently.^[16] It was found that dendritic encapsulation does not prevent Zn²⁺-porphyrin ligation, and the equilibrium constants *K* for the binding of different ligands was measured. The core porphyrins have a planar conformation of the macrocycle in the four-coordinate (unligated) form, and a dome-type nonplanar distortion is observed for the ligated forms.^[29] Interactions of the dendritic shell with the porphyrin core would depend on the conformational state of the porphyrin. Therefore, it seems reasonable to analyze the spectroscopic data for the four- and five-coordinate dendrimer core separately (Tables 1 and 2, respectively).

The formation of dendrimers results in small long-wavelength shifts of the absorption bands (compounds **B** and **E** compared to parent **ZnTPP**, or compounds **C** and **F** compared to parent **ZnTMesP**). These changes take place simultaneously with changes in the ratio of the intensities of the pure electronic band to the vibronic band in both absorbance ($A_{0,0}/A_{1,0}$) and fluorescence ($F_{0,0}/F_{0,1}$) spectra (Table 1). The $A_{0,0}/A_{1,0}$ value is related to the ratio of the transition dipole moments of these transitions. On the other hand, this ratio is proportional to the square of the energy difference between the two one-electron configurations: $A_{0,0}/A_{1,0} \approx [{}^1E(a_{2u}, e_g) - {}^1E(a_{1u}, e_g)]^2$, and is used as a measure of the energy mismatch between the highest occupied molecular orbitals (HOMOs) a_{2u} and a_{1u} (D_{4h} symmetry notation).^[30] Both the long wavelength band shift and increase in the $A_{0,0}/A_{1,0}$ ratio are likely to result from electron density transferring from the dendrons to the macrocycle. This leads to a slight increase in the electron density at the *meso*-carbon atoms of the porphyrin, thus increasing the energy of the a_{2u} MO. The more separated in energy a_{2u} and a_{1u} orbitals are, the higher the absorption of the 0,0 transition is.^[30]

A similar trend was also observed when the spectroscopic data for all dendrimers studied (in both four- and five-coordinate forms of porphyrin core) were compared. A simple rationale for such a behavior lies in the relationship of the spectral pattern and the type of the nearest aryl ring to the *meso*-carbon spacer. The $A_{0,0}/A_{1,0}$ value is different for parent **ZnTPP** and **ZnTMesP** porphyrins and may be related to the position of the aryl ring relative to the mean macrocycle plane, which modulates the strength of the electronic communication between them. In the case of mesityl substitution, the dihedral angle θ is 90° due to steric hin-

drance induced by two *ortho*-methyl groups, and it is approximately 60–70° in the case of phenyl substitution because relatively little steric interaction occurs.^[31] In the dendrimers, these features give rise to substantial differences in the $A_{0,0}/A_{1,0}$ ratio between compounds **B** and **E** (both having all four unhindered spacers) from one side, and **C** and **F** (both having all four hindered spacers) from the other.

Table 3 indicates the Soret band maxima for all the studied dendrimers. It can be seen that the spectral shift of the Soret bands follow the same trend for both ligated (in THF) and nonligated (in CH₂Cl₂) dendrimers. The energy of the B band (Soret) can be fitted as a linear function of the Q band energy in both sets of data. This fact indicates that the effects of both dendritic encapsulation and axial ligation can be monitored with either the Q- or B-band regions without any loss of information. The mean difference between the B- and Q-band energies for all the studied dendrimers is $6700 \pm 90 \text{ cm}^{-1}$, which is in excellent agreement with the data reported for the series of metallocomplexes of TPP.^[30a]

Table 3. Soret band maxima for the studied compounds in CH₂Cl₂ and THF.

	λ_{B} [nm]	
	CH ₂ Cl ₂	THF
A	420.0	424.5
B	420.0	424.5
C	423.5	428.5
D	420.0	424.5
E	420.0	425.0
F	423.5	428.5

The gradual spectral evolution in the *meso*-substituted porphyrin-indolocarbazole conjugates when the substitution pattern changes in the series as B₄, AB₃, ABAB, AABB, A₃B (A = indolocarbazole fragment attached via phenyl spacer, B = mesityl) has been explained recently.^[32] By applying this approach to the case under consideration, the relationship between the spectral pattern and the type of the nearest aryl ring to the *meso*-carbon spacer is revealed (Figure 2). The ground state absorption spectrum of dendrimers with the same type of dendrons depends on the *meso*-spacer type, with the phenyl spacer allowing the highest absorptivity of the 0,0 transition band, and the mesityl

spacer the lowest. The reverse is true for the 1,0 band position (Tables 1 and 2).

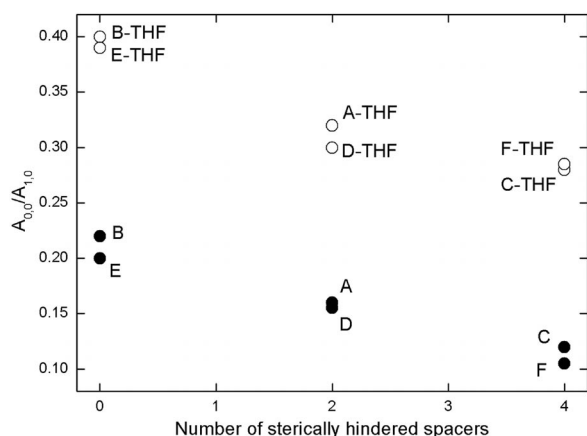


Figure 2. Correlation between the $A_{0,0}/A_{1,0}$ ratio and the number of sterically hindered spacers in the studied compounds with the four-coordinate form of the Zn-porphyrin core (closed circles, A–F), and with the five-coordinate form of the Zn-porphyrin core (open circles, A-THF–F-THF).

In the case of a pure electronic substitution effect, the $A_{0,0}/A_{1,0}$ ratio is known to be reciprocal to the energy of the 0,0 band for tetra-aryl-porphyrins.^[30,33] Since, for such porphyrins, the relation ${}^1E(a_{2u}, e_g) < {}^1E(a_{1u}, e_g)$ holds, decrease in the energy of the one-electron configuration simultaneously leads to larger splitting ${}^1E(a_{2u}, e_g) - {}^1E(a_{1u}, e_g)$.^[33] Therefore, when dome-type nonplanar distortions are induced (the degree of which depends on the ligand basicity, i.e., pyridine induces higher nonplanar distortions compared with THF^[34]) in going from four- to five-coordinate compounds, a long-wavelength shift of the absorption spectrum takes place. There is no linear correlation over the whole set of data (Figure 3) since the ligands have their own electronic contribution.

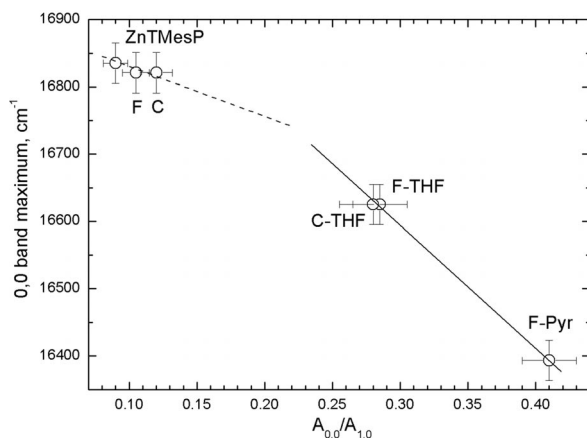


Figure 3. Correlation between the long-wavelength (0,0) band maximum in the absorption spectra and the $A_{0,0}/A_{1,0}$ ratio for dendrimers with four sterically hindered spacers.

The Stokes shift $\Delta\lambda_{\text{Stokes}} = \lambda_{0,0}^{\text{abs}} - \lambda_{0,0}^{\text{fl}}$ can be considered as an estimate of the conformational flexibility/degree of freedom for tetrapyrrolic compounds.^[34,35] Therefore,

based on the $\Delta\lambda_{\text{Stokes}}$ value behavior in dendrimers, the influence of the dendritic shell on the intrinsic conformational flexibility of the porphyrin core could be estimated. In the case of a four-coordinate porphyrin core, the $\Delta\lambda_{\text{Stokes}}$ values remain practically unchanged for dendrimers **B** and **E** (“ZnTPP-like”), but a decrease of the Stokes shift was shown in the case of “ZnTMesP-like” dendrimers **C** and **F** (Table 4). A substantial decrease in the $\Delta\lambda_{\text{Stokes}}$ value takes place upon ligation in both parent porphyrins and dendrimers. About the same reduction of ca. 100 cm^{-1} is found for both ZnTPP porphyrin and dendrimers **B** and **E**, indicating that the dendrimer/core interactions do not alter the intrinsic conformational changes occurring upon the axial ligation. Axial ligation of sterically hindered ZnTMesP leads to about a threefold decrease in the $\Delta\lambda_{\text{Stokes}}$ value down to ca. 80 cm^{-1} , irrespective of the type of ligand. One can suggest that ZnTMesP-L possesses a quite rigid molecular conformation. In the case of “ZnTMesP-like” ligated dendrimers **C-THF** and **F-THF**, the same value of the Stokes shift is found. This means that neither ligand free (in CH_2Cl_2) nor ligated (in THF) porphyrin core undergoes noticeable restrictions from the dendritic shell to adopt a dome-type conformation. A slightly higher value was measured for **F-Pyr** dendrimer, but the differences were too small for unambiguous interpretation.

Table 4. Stokes shift values for four- and five-coordinate forms of the Zn-porphyrin core of dendrimers A–F.

Compound	$\Delta\lambda_{\text{Stokes}}$ [cm^{-1}]	Compound	$\Delta\lambda_{\text{Stokes}}$ [cm^{-1}]
A	228	A-THF	154
B	287	B-THF	196
C	171	C-THF	83
D	228	D-THF	154
E	285	E-THF	196
F	171	F-THF	83
		F-Pyridine	122
ZnTPP	272	ZnTPP-THF	154
		ZnTPP-Pyridine	177
ZnTMesP	230	ZnTMesP-THF	71
		ZnTMesP-Pyridine	82

Luminescent Properties

All the studied dendrimers are luminescent molecules possessing dual emission (Figure 4): the $S_1 \rightarrow S_0$ fluorescence and the fluorescence from higher excited states, namely, $S_2 \rightarrow S_0$ fluorescence, which is frequently also named blue fluorescence.^[36] Thus, the dendrimers provide a dual red and blue luminescent response.

The $S_1 \rightarrow S_0$ and $S_2 \rightarrow S_0$ fluorescence differ in their lifetimes. Whereas the S_1 state lifetime was found to be around 2 ns (Table 5), the S_2 state lifetime for Zn-tetraarylporphyrins was three orders of magnitude shorter, i.e., 1.5–3 ps.^[36,37] As a result of such a short lifetime, blue $S_2 \rightarrow S_0$ fluorescence should be practically insensitive to the slow conformational dynamics in dendrimers. The main photophysical parameters for the lowest singlet S_1 state of the

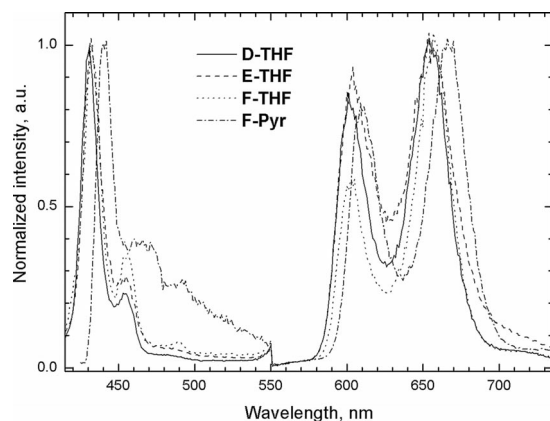


Figure 4. Total luminescence spectra of compounds **D-THF**–**F-THF** (spectra of porphyrins **A-THF**–**C-THF** are not shown, since compounds **A** and **D**, **B** and **E**, **C** and **F** are spectrally indistinguishable in pairs, see Tables 1, 2, 3, and 4, and 6). The blue $S_2 \rightarrow S_0$ fluorescence spectra ($\lambda_{\text{exc}} = 400$ nm for all the compounds, with the exception of **F-Pyr**, where $\lambda_{\text{exc}} = 410$ nm; $\lambda_{\text{em}} = 415$ – 550 nm) are normalized for the intensity of the electronic (0,0) band, and the red $S_1 \rightarrow S_0$ fluorescence spectra ($\lambda_{\text{exc}} = 545$ nm; $\lambda_{\text{em}} = 550$ – 740 nm) are normalized for the intensity of the vibronic (0,1) band. Spectra measured in CH_2Cl_2 are shown in the Supporting Information.

compounds studied are listed in Table 5. All of them reveal differences between the four- and five-coordinate forms of the Zn-porphyrin core. Therefore, we performed the analysis for the four-coordinate core dendrimers first and then compared these values with those for the ligated dendrimers. The emission rate constant k_{fl} increased upon formation of dendrimers compared with the parent core porphyrins. Thus, the k_{fl} value in dendrimers **C** and **F** is about 30% higher than those of **ZnTMesP**, and the k_{fl} value in dendrimers **B** and **E** is about 20% higher than the parent **ZnTPP**. In addition, the radiationless rate constant k_{nr} remains practically unchanged upon dendrimer formation (see Table 5). As a result, the fluorescence quantum yield Φ_{fl} increases noticeably in dendrimers, reaching 0.038–0.043 compared to 0.032–0.033 for the parent core porphyrins. Dendrimers **A** and **D** show intermediate k_{fl} and k_{nr} values, which also leads to an increase in the fluorescence quantum yield Φ_{fl} of the same order of magnitude as those of dendrimers **B** and **E**. Thus, the $S_1 \rightarrow S_0$ fluorescence response quantum yield is maximal in dendrimers **C** and **F**.

Formation of a five-coordinate dendrimer core ($L = \text{THF}$) brings about changes in the k_{fl} and k_{nr} rate constants. The k_{fl} value decreases slightly for dendrimers **C** and **F**, and remains about the same for dendrimers **B** and **E**. It is interesting to note that the value of the emission rate constant k_{fl} for “**ZnTPP**-like” and “**ZnTMesP**-like” dendrimers is roughly the same as for the parent core porphyrins after ligation with THF. Radiationless deactivation rate constant k_{nr} undergoes minor changes in all cases, except for a decrease in dendrimers **A** and **D**. All these changes lead to a decrease in the fluorescence quantum yield of dendrimers **C** and **F**, and an increase in Φ_{fl} for dendrimers **A** and **D**.

An increase in both k_{fl} and k_{nr} rate constants is observed when the core of dendrimer **F** is ligated with pyridine. As a result, the fluorescence quantum yield Φ_{fl} slightly decreases, since the probability of radiationless deactivation increases. Ligation with pyridine is found to lead to very similar fluorescence quantum yields in all the studied compounds. It could be suggested that internal radiationless conversion may account for the increase in the k_{nr} value upon the formation of axially ligated compounds upon the formation of a dome type nonplanar conformer, since intersystem crossing is expected to be barely affected.^[34a]

The emission rate constant k_{fl} and radiationless deactivation rate constant k_{nr} behavior can be rationalized in terms of the degree of steric hindrance induced by *meso*-aryl spacers, as done above when analyzing the ground-state absorption spectra. Two correlation plots are presented in Figure 5. The “**ZnTPP**-like” dendrimers **B** and **E** do not show substantial differences in either k_{fl} or k_{nr} values when going from the four- to five-coordinate dendrimer core. Dendrimers **A** and **D**, which follow the *trans*- $\text{Ph}_2\text{-Mes}_2$ pattern in architecture, maintain approximately the same k_{fl} value, but the k_{nr} value reduces substantially upon dendrimer core ligation. Finally, in “**ZnTMesP**-like” dendrimers **C** and **F**, the radiationless deactivation probability k_{nr} does not undergo large changes, but their k_{fl} values decrease remarkably upon ligand attachment. Therefore, the fluorescence quantum yield Φ_{fl} remains about the same in dendrimers **B** and **E**, slightly increases in dendrimers **A** and **D**, and decreases noticeably in dendrimers **C** and **F**. Thus, one can suggest that dendrimer architectures with all four *meso*-aryl spacers providing a degree of steric hindrance are most appropriate to monitor the processes related to the axial ligation of the

Table 5. Luminescent properties for the S_1 state of dendrimers **A**–**F**.

	$\Phi_{\text{fl}} \times 10^2$	Four-coordinate core			$\Phi_{\text{fl}} \times 10^2$	Five-coordinate core ^[a]		
		τ_{fl} [ns]	$k_{\text{fl}}, 10^7 \text{ s}^{-1}$	$k_{\text{nr}}, 10^8 \text{ s}^{-1}$		τ_{fl} [ns]	$k_{\text{fl}}, 10^7 \text{ s}^{-1}$	$k_{\text{nr}}, 10^8 \text{ s}^{-1}$
A	3.8	1.98	1.92	4.86	4.0	2.33	1.79	4.11
B	3.8	1.67	2.28	5.76	3.7	1.68	2.20	5.73
C	3.9	2.30	1.70	4.18	3.7	2.44	1.52	3.95
D	3.8	1.99	1.91	4.83	4.3	2.25	1.91	4.25
E	3.8	1.70	2.24	5.66	3.9	1.72	2.27	5.59
F	4.3	2.36	1.82	4.06	3.6/3.4	2.46/1.96	1.46/1.74	3.92/4.93
ZnTPP	3.3	1.75	1.89	5.53	3.3/3.2	1.54/1.81	2.14/1.77	6.28/5.35
ZnTMesP	3.2	2.33	1.37	4.15	3.6/3.3	2.42/1.92	1.49/1.72	3.98/5.04

[a] Data for $L = \text{THF}$ and $L = \text{Pyr}$ are given in the nominator and denominator, respectively.

dendrimer core, since they provide larger luminescence response differences between the four- and five-coordinate dendrimer core (Table 6).

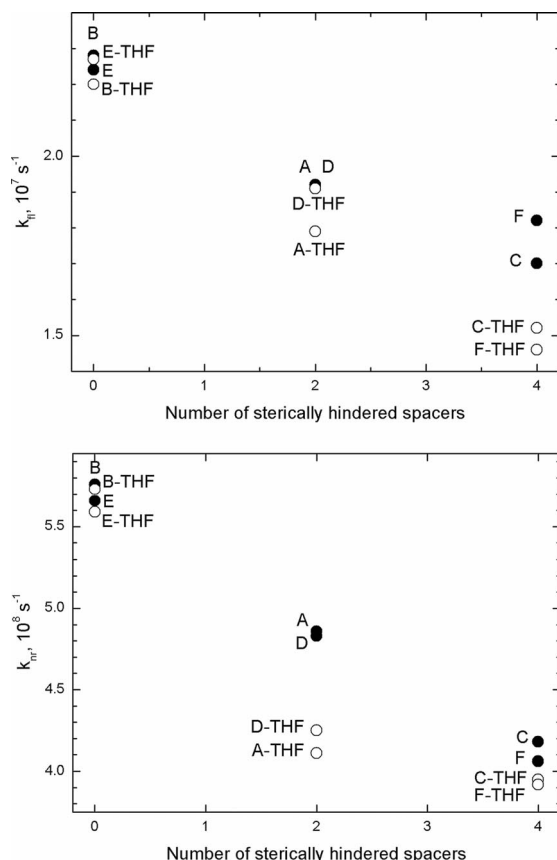


Figure 5. Correlation between the rate constant of emissive (k_{ri} , upper panel) and total radiationless (k_{nr} , lower panel) deactivation of lowest singlet S_1 state and the number of sterically hindered spacers in the studied compounds with the four-coordinate form of the Zn-porphyrin core (closed symbols, A–F), and with the five-coordinate form of the Zn-porphyrin core (open symbols, A-THF–F-THF).

Table 6. Luminescent properties for the S_2 state of dendrimers A–F.

	$\lambda_{0,0}^{fl}$ [nm]	$\lambda_{0,1}^{fl}$ [nm]	$\Phi_{fl}^B \times 10^3$
A-THF	431.0	454.0	0.92
B-THF	432.0	455.0	1.11
C-THF	432.5	455.5	0.78
D-THF	431.0	454.0	1.10
E-THF	432.0	455.0	1.09
F-THF	432.5	455.5	0.79
F-Pyr	440.5	466.5	0.41
ZnTPP	427.0	–	1.25
ZnTPP-THF	430.0	454.0	1.10
ZnTPP-Pyridine	439.0	472.0	0.60
ZnTMesP	427.5	–	0.85
ZnTMesP-THF	428.0	455.0	1.31
ZnTMesP-Pyridine	438.0	472.0	0.53

Parameters of the blue $S_2 \rightarrow S_0$ fluorescence for the studied compounds are presented in Table 5. The positions of the blue fluorescence spectrum follow the trend for the

absorption spectrum. There is a long-wavelength shift on going from compounds that have the dendrimer core ligated with THF to those with pyridine as a ligand. The fluorescence quantum yields Φ_{fl}^B are of the same order of magnitude in the four studied dendrimers A-THF, B-THF, D-THF, and E-THF. However, there is a small decrease in Φ_{fl}^B for “ZnTMesP-like” dendrimers C-THF and F-THF. The Φ_{fl}^B value decreases further upon ligation of dendrimer F with pyridine.

The quantum yield of the blue $S_2 \rightarrow S_0$ fluorescence depends on the competition between the radiationless internal $S_2 \rightarrow S_1$ conversion and the $S_2 \rightarrow S_0$ radiative transition rate constants.^[36] The radiationless internal $S_2 \rightarrow S_1$ conversion is much higher than the $S_2 \rightarrow S_0$ radiative transition rate and this results in a very low blue fluorescence quantum yield Φ_{fl}^B . Therefore, to a good approximation, Φ_{fl}^B can be taken as the simple ratio $k_{fl}(S_2 \rightarrow S_0)/k_{IC}(S_2 \rightarrow S_1)$. For the TPP metallocomplexes, the internal conversion rate $k_{IC}(S_2 \rightarrow S_1)$ is known to be reciprocal to the energy gap $\Delta E(S_2 - S_1)$.^[38] The plot of the Φ_{fl}^B value as a function of the $S_2 - S_1$ energy gap (Figure 6) demonstrates a good linear correlation in the series consisting of the parent ZnTPP and ZnTMesP porphyrins (both four-coordinate and ligated with THF and pyridine) and the ligated dendrimers A-THF–F-THF, and F-Pyr. Such a correlation may be explained by changes in the internal conversion rate constant $k_{IC}(S_2 \rightarrow S_1)$ due to variation of the energy gap $\Delta E(S_2 - S_1)$, whereas the radiative transition rate constant $k_{fl}(S_2 \rightarrow S_0)$ remains about the same. It is worthwhile to note that essentially the same behavior is observed for both four- and five-coordinate (with THF and pyridine) compounds. The differences in the rotational degree of freedom for *meso*-substituents/dendrons in the ZnTPP and “ZnTPP-like” dendrimers B and E, the ZnTMesP and “ZnTMesP-like” dendrimers C and F, and the *trans*-Ph₂-Mes₂ pattern dendrimers A and D, also have no noticeable influence on either the internal conversion rate $k_{IC}(S_2 \rightarrow S_1)$ or radiative transition rate $k_{fl}(S_2 \rightarrow S_0)$.

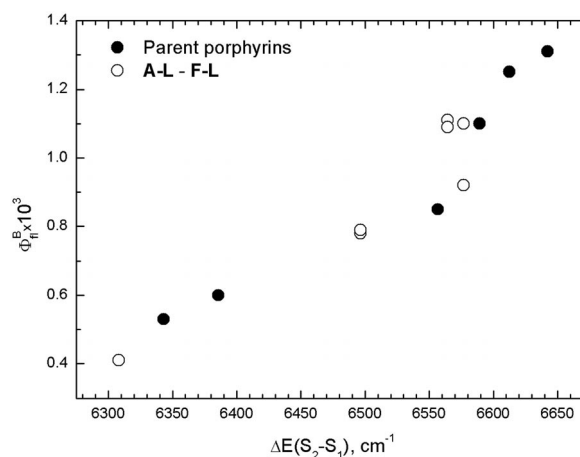


Figure 6. Correlation between the blue $S_2 \rightarrow S_0$ fluorescence quantum yield Φ_{fl}^B and the energy gap $\Delta E(S_2 - S_1)$ for dendrimers A–F and parent porphyrins.

Conclusions

The spectral luminescent properties of the family of Zn-porphyrin core dendrimers with triazole-linked carbazole dendrons have been studied. The dual emission of the dendrimers in the blue and red regions has been observed and characterized in detail. It was found that the spectral properties of new dendrimers retain the main features of the parent core porphyrins. The observed trends in the spectroscopic data and photophysical properties of the dendrimers have been rationalized in terms of the type of *meso*-spacer between the macrocycle and dendritic shell. The key feature of the *meso*-spacer is expected to be the degree of hindrance for aryl ring rotation relative to the mean porphyrin plane. Based on the observed differences in the $S_1 \rightarrow S_0$ fluorescence quantum yield upon going from four- to five-coordinate dendrimers, the mesityl-like dendrimer architecture is expected to be optimal for sensor design due to the largest changes in the luminescent signal upon porphyrin core ligation. The blue $S_2 \rightarrow S_0$ fluorescence quantum yield values for dendrimers can be rationalized in terms of the $S_2 \rightarrow S_1$ energy gap law.

Experimental Section

General Experimental Methods: NMR spectra were acquired with Bruker Avance 300 MHz, Bruker AMX 400 MHz or Bruker Avance II⁺ 600 MHz spectrometers, and chemical shifts (δ) are reported in parts per million (ppm) referenced to tetramethylsilane (TMS) or the internal (NMR) solvent signals. Mass spectra were recorded with a HP5989A apparatus (CI and EI, 70 eV ionization energy) with an Apollo 300 data system or with a Thermo Finnigan LCQ Advantage apparatus (ESI). Exact mass measurements were acquired with a Kratos MS50TC instrument (performed in the EI mode at a resolution of 10000). Melting points (not corrected) were determined with a Reichert Thermovar apparatus. For column chromatography, 70–230 mesh silica 60 (E. M. Merck) was used as the stationary phase. Chemicals received from commercial sources were used without further purification. Gel permeation chromatography (GPC) was used to determine the polydispersity index (PDI) of all dendrimers A–F; a Shimadzu 10A apparatus was used with a Plgel 5 μ m mixed-D column and all measurements were performed in THF as eluent against polystyrene standards. Infrared spectra were recorded with an Alpha FTIR spectrometer. MALDI-TOF mass spectrometry was carried out with a Bruker Daltonics – ultraflex II & ultraflex II TOF/TOF using the matrix 2,5-dihydroxybenzoic acid for all samples.

Spectroscopic Methods and Instrumentation: UV/Vis spectra were recorded with a Perkin–Elmer Lambda 20 or Cary Varian spectrophotometer. The fluorescence spectra and fluorescence excitation spectra were measured with an SFL-1211 spectrofluorimeter (JSC Solar). The fluorescence decay kinetics were measured with an in-house constructed single-photon counting spectrometer (KU Leuven). The OPA, pumped with a mode-locked Ti:sapphire laser (Tsunami, Spectra Physics), was used as excitation source. The linearly polarized excitation light was rotated to a vertical direction by the use of a Berek compensator (New Focus) in combination with a polarization filter and directed onto the sample. The emission spectra were collected at 90° with respect to the incident light and guided through a polarization filter that was set at the magic angle (54.7°) with respect to the polarization of the excitation

beam. The fluorescence was spectrally resolved by a monochromator (Sciencetech 9030, 6 mm bandwidth), and detected by a micro-channel plate photomultiplier tube (MCP-PMT, R3809U, Hamamatsu). A time-correlated Single Photon Timing PC module (SPC 830, Becker & Hickl) was used to obtain the fluorescence decay histogram in 4096 channels. The decays were recorded with 10,000 counts in the peak channel, in time windows of 25 ns corresponding to 6.1 ps/channel and analyzed globally with a time-resolved fluorescence analysis (TRFA) software. The full-width at half-maximum (FWHM) of the IRF was typically in the order of 32 ps. The quality of the fits was judged by the fit parameters χ^2 (< 1.2), $Z\chi^2$ (< 3) and the Durbin Watson parameter ($1.8 < DW < 2.2$) as well as by visual inspection of the residuals and autocorrelation function.

The absorbance and fluorescence measurements were conducted in standard rectangular cells (1 × 1 cm, Hellma) in air-equilibrated solutions at 293 ± 2 K. Deoxygenated solutions were used for measurements of the fluorescence quantum yield and lifetime. Deoxygenation of the solutions was performed by argon bubbling for 20 min immediately before measurements. The fluorescence quantum yield Φ_f was determined by using standard sample methods, with the Zn-5,10,15,20-tetraphenylporphyrin (Zn-TTP) taken as a standard sample ($\Phi_f^0 = 0.033$).

3,5-Bis(azidomethyl)-2,4,6-trimethylbenzaldehyde (4): Yellow oil. ¹H NMR (300 MHz, CDCl₃, 25 °C, TMS): δ = 10.62 (s, 1 H, CHO), 4.50 (s, 4 H, 2 × CH₂), 2.54 (s, 6 H, 2 × CH₃), 2.49 (s, 3 H, CH₃) ppm. ¹³C NMR (75 MHz, CDCl₃, 25 °C, TMS): δ = 195.31 (CHO), 142.24 (C-Ar), 139.15 (2 × C-Ar), 134.16 (C-Ar), 131.62 (2 × C-Ar), 48.11 (2 × CH₂), 16.90 (CH₃), 15.98 (2 × CH₃) ppm. HRMS (EI): *m/z* calcd. for C₁₂H₁₄N₆O 258.1229; found 232.1110 [MH⁺ – N₂].

1-[(Trimethylsilyl)ethynyl]-3,5-bis[3,6-bis(tert-butyl)carbazol-9-yl]benzene (11): White solid; m.p. 320–322 °C. ¹H NMR (300 MHz, CDCl₃, 25 °C, TMS): δ = 8.13 (d, ⁴J_{H,H} = 0.93 Hz, 4 H, Ar-H), 7.75 (d, ⁴J_{H,H} = 1.71 Hz, 1 H, Ar-H), 7.73 (d, ⁴J_{H,H} = 1.71 Hz, 2 H, Ar-H), 7.49 (dd, ⁴J_{H,H} = 1.71, ³J_{H,H} = 8.67 Hz, 4 H, Ar-H), 7.45 (d, ³J_{H,H} = 8.46 Hz, 4 H, Ar-H), 1.46 (s, 36 H, tert-butyl), 0.27 (s, 9 H) ppm. ¹³C NMR (75 MHz, CDCl₃, 25 °C, TMS): δ = 128.24, 124.85, 123.99, 116.54, 109.29 (CH-Ar), 143.56, 139.91, 138.92, 126.46, 123.81 (C-Ar), 103.35, 97.03 (C≡C), 34.91 (C, tert-butyl), 32.13 (CH₃, tert-butyl) ppm. MALDI-TOF: *m/z* calcd. for C₅₁H₆₀N₂Si [M⁺] 728.45; found 728.29.

1-Ethynyl-3,5-bis[3,6-bis(tert-butyl)carbazol-9-yl]benzene (12): White solid; m.p. > 350 °C. ¹H NMR (300 MHz, CDCl₃, 25 °C, TMS): δ = 8.14 (s, 4 H, H-carbazole), 7.80 (s, 1 H, Ar-H), 7.76 (s, 2 H, Ar-H), 7.47 (ddd, 8 H, H-carbazole), 3.21 (s, 1 H, C≡CH), 1.46 (s, 36 H, tert-butyl) ppm. ¹³C NMR (75 MHz, CDCl₃, 25 °C, TMS): δ = 128.13, 124.92, 123.89, 116.40, 109.12 (CH-Ar), 143.52, 139.93, 138.71, 125.22, 123.72 (C-Ar), 82.10, 79.35 (C≡C), 34.75 (C, tert-butyl), 31.97, 32.13 (CH₃, tert-butyl) ppm. HRMS (EI): *m/z* calcd. for C₄₈H₅₂N₂ 656.4130; found 656.4120.

5,15-Bis(2,4,6-trimethylphenyl)-10,20-bis(4-azidomethylphenyl)porphyrin (7): Purple solid. ¹H NMR (300 MHz, CDCl₃, 25 °C, TMS): δ = 8.76 (d, ³J_{H,H} = 4.53 Hz, 4 H, H-pyrrole), 8.69 (d, ³J_{H,H} = 4.71 Hz, 4 H, H-pyrrole), 8.23 (d, ³J_{H,H} = 7.71 Hz, 4 H, Ar-H), 7.67 (d, ³J_{H,H} = 7.89 Hz, 4 H, Ar-H), 7.27 (s, 4 H, H-mesityl), 4.68 (s, 4 H, 2 × CH₂), 2.61 (s, 6 H, 2 × CH₃), 1.83 (s, 12 H, 4 × CH₃), –2.61 (s, 2 H, 2 × NH) ppm. ¹³C NMR (75 MHz, CDCl₃, 25 °C, TMS): δ = 134.83, 127.77, 126.49 (CH-Ar), 142.07, 139.37, 138.35, 137.77, 118.60, 118.48 (C-Ar), 54.87 (CH₂), 21.62 (4 × CH₃), 21.45 (2 × CH₃) ppm. MALDI-TOF: *m/z* calcd. for C₅₂H₄₄N₁₀ 808.375; found 808.145.

5,10,15,20-Tetrakis[3,5-bis(azidomethyl)-2,4,6-trimethylphenyl]porphyrin (9): Purple solid. ^1H NMR (300 MHz, CDCl_3 , 25 °C, TMS): δ = 8.56 (s, 8 H, H-pyrrole), 4.72 (s, 16 H, $8 \times \text{CH}_2$), 2.78 (s, 12 H, $4 \times \text{CH}_3$), 1.93 (s, 24 H, $8 \times \text{CH}_3$), -2.38 (s, 2 H, $2 \times \text{NH}$) ppm. ^{13}C NMR (75 MHz, CDCl_3 , 25 °C, TMS): δ = 140.24, 140.12, 138.10, 129.85, 118.36 (C-Ar), 49.14 (CH_2), 19.49 ($2 \times \text{CH}_3$), 16.54 (CH_3) ppm. MALDI-TOF: m/z calcd. for $\text{C}_{64}\text{H}_{62}\text{N}_{28}$ 1222.571; found 1222.561.

Zn^{II}-5,15-bis(2,4,6-trimethylphenyl)-10,20-bis(4-azidomethylphenyl)porphyrin: Purple solid. ^1H NMR (300 MHz, $[\text{D}_8]\text{THF}$, 25 °C, TMS): δ = 8.76 (d, $^3J_{\text{H,H}} = 4.71$ Hz, 4 H, H-pyrrole), 8.65 (d, $^3J_{\text{H,H}} = 4.71$ Hz, 4 H, H-pyrrole), 8.21 (d, $^3J_{\text{H,H}} = 7.89$ Hz, 4 H, Ar-H), 7.72 (d, $^3J_{\text{H,H}} = 7.92$ Hz, 4 H, Ar-H), 7.28 (s, 4 H, H-mesityl), 4.75 (s, 4 H, $2 \times \text{CH}_2$), 2.59 (s, 6 H, $2 \times \text{CH}_3$), 1.84 (s, 12 H, $4 \times \text{CH}_3$) ppm. ^{13}C NMR (75 MHz, $[\text{D}_8]\text{THF}$, 25 °C, TMS): δ = 135.58, 132.63, 130.82, 128.47, 126.97 (CH-Ar), 150.75, 150.64, 144.31, 140.65, 139.85, 138.07, 136.04, 120.25, 119.39 (C-Ar), 55.34 (CH_2), 21.94 ($4 \times \text{CH}_3$), 21.56 ($2 \times \text{CH}_3$) ppm. MALDI-TOF: m/z calcd. for $\text{C}_{52}\text{H}_{42}\text{N}_{10}\text{Zn}$ 870.29; found 870.22.

Zn^{II}-5,10,15,20-tetrakis[3,5-bis(azidomethyl)-2,4,6-trimethylphenyl]porphyrin: Purple solid. ^1H NMR (300 MHz, $[\text{D}_8]\text{THF}$, 25 °C, TMS): δ = 8.56 (s, 8 H, H-pyrrole), 4.79 (s, 16 H, $8 \times \text{CH}_2$), 2.80 (s, 12 H, $4 \times \text{CH}_3$), 1.94 (s, 24 H, $8 \times \text{CH}_3$) ppm. ^{13}C NMR (75 MHz, $[\text{D}_8]\text{THF}$, 25 °C, TMS): δ = 150.63, 142.57, 140.67, 138.61, 130.98, 119.57 (C-Ar), 131.48 (CH-pyrrole), 49.81 (CH_2), 19.62 ($2 \times \text{CH}_3$), 16.52 (CH_3) ppm. MALDI-TOF: m/z calcd. for $\text{C}_{64}\text{H}_{60}\text{N}_{28}\text{Zn}$ 1284.484; found 1285.497 [$\text{M} + \text{H}^+$].

Dendrimer A: Purple solid. ^1H NMR (600 MHz, CDCl_3 , 25 °C, TMS): δ = 8.84 (d, $^3J_{\text{H,H}} = 4.44$ Hz, 4 H, H-pyrrole), 8.78 (d, $^3J_{\text{H,H}} = 4.38$ Hz, 4 H, H-pyrrole), 8.27 (d, $^3J_{\text{H,H}} = 7.68$ Hz, 4 H, Ar-H), 8.15 (s, 4 H, H-carbazole), 8.10 (d, $^3J_{\text{H,H}} = 8.28$ Hz, 4 H, Ar-H), 8.08 (s, 2 H, H-triazole), 7.68 (d, $^3J_{\text{H,H}} = 8.28$ Hz, 4 H, Ar-H), 7.66 (d, $^3J_{\text{H,H}} = 8.22$ Hz, 4 H, Ar-H), 7.48 (d, $^3J_{\text{H,H}} = 7.14$ Hz, 4 H, Ar-H), 7.40 (d, $^3J_{\text{H,H}} = 8.28$ Hz, 4 H, Ar-H), 7.27 (s, 4 H, H-mesityl), 5.96 (s, 4 H, $2 \times \text{CH}_2$), 2.62 (s, 6 H, $2 \times \text{CH}_3$), 1.81 (s, 12 H, $4 \times \text{CH}_3$), 1.47 (s, 36 H, *tert*-butyl) ppm. ^{13}C NMR (150 MHz, CDCl_3 , 25 °C, TMS): δ = 135.11, 132.15, 131.04, 127.73, 127.23, 127.12, 126.16, 123.70, 119.93, 116.30, 109.27 (CH-Ar), 150.12, 149.93, 147.92, 143.55, 143.07, 139.24, 139.22, 138.89, 138.21, 137.62, 133.98, 129.29, 119.64, 119.22 (C-Ar), 54.40 (CH_2), 34.77 (C, *tert*-butyl), 32.04 (CH_3 , *tert*-butyl), 21.62 (CH_3), 21.46 (CH_3) ppm. MALDI-TOF: m/z calcd. for $\text{C}_{108}\text{H}_{100}\text{N}_{12}\text{Zn}$ 1628.748 [M^+], 1600.748 [$\text{M} - 28$]; found 1629.629 [$\text{M} + \text{H}^+$], 1600.714 [$\text{M} - 28$]. Polydispersity index (PDI) = 1.024.

Dendrimer B: Purple solid. ^1H NMR (400 MHz, CDCl_3 , 25 °C, TMS): δ = 8.85 (s, 8 H, H-pyrrole), 8.13 (s, 16 H, Ar-H), 7.73 (s, 4 H, H-triazole), 7.68 (d, $^3J_{\text{H,H}} = 7.04$ Hz, 8 H, Ar-H), 7.50 (d, $^3J_{\text{H,H}} = 8.2$ Hz, 8 H, Ar-H), 7.41 (d, $^3J_{\text{H,H}} = 8.24$ Hz, 16 H, Ar-H), 7.30 (d, $^3J_{\text{H,H}} = 8.6$ Hz, 8 H, Ar-H), 5.62 (s, 8 H, $2 \times \text{CH}_2$), 1.43 (s, 72 H, *tert*-butyl) ppm. ^{13}C NMR (100 MHz, CDCl_3 , 25 °C, TMS): δ = 150.08, 147.43, 143.56, 143.09, 139.07, 138.04, 135.05, 133.86, 131.96, 128.67, 127.06, 126.89, 125.82, 123.69, 123.50, 120.16, 119.97, 116.31, 109.22 (C and CH-Ar), 54.03 (CH_2), 34.73 (C, *tert*-butyl), 32.01 (CH_3 , *tert*-butyl) ppm. MALDI-TOF: m/z calcd. for $\text{C}_{160}\text{H}_{148}\text{N}_{20}\text{Zn}$ 2413.148 [M^+], 2385.148 [$\text{M} - 28$]; found 2415.042 [$\text{M} + 2\text{H}^+$], 2385.120 [$\text{M} - 28$]. Polydispersity index (PDI) = 1.015.

Dendrimer C: Purple solid. ^1H NMR (400 MHz, CDCl_3 , 25 °C, TMS): δ = 8.70 (s_{bb} , 8 H, H-pyrrole), 8.13 (s, 16 H, H-carbazole), 8.01 (d, $^3J_{\text{H,H}} = 7.04$ Hz, 16 H, Ar-H), 7.72 (s, 8 H, H-triazole), 7.56 (d, $^3J_{\text{H,H}} = 8.24$ Hz, 16 H, Ar-H), 7.38 (d, $^3J_{\text{H,H}} = 7.04$ Hz, 16 H, Ar-H), 7.31 (d, $^3J_{\text{H,H}} = 8.6$ Hz, 16 H, Ar-H), 5.69 (s_{bb} , 16 H, CH_2), 2.50 (s_{bb} , 12 H, $4 \times \text{CH}_3$), 1.90 (s_{bb} , 24 H, $8 \times \text{CH}_3$), 1.42 ppm

(s, 144 H, *tert*-butyl) ppm. ^{13}C NMR (100 MHz, CDCl_3 , 25 °C, TMS): δ = 131.34, 127.14, 126.92, 123.76, 119.46, 116.29, 109.16 (CH-Ar), 149.85, 147.05, 143.15, 141.79, 141.20, 138.98, 138.50, 138.08, 129.17, 129.05, 123.48, 118.96 (C-Ar), 49.36 (CH_2), 34.72 (C, *tert*-butyl), 31.99 (CH_3 , *tert*-butyl), 19.75 (CH_3), 16.40 (CH_3) ppm. MALDI-TOF: m/z calcd. for $\text{C}_{288}\text{H}_{292}\text{N}_{36}\text{Zn}$: 4318.324 [M^+]; found 4320.7 [$\text{M} + 2\text{H}^+$]. Polydispersity index (PDI) = 1.037.

Dendrimer D: Purple solid. ^1H NMR (400 MHz, CDCl_3 , 25 °C, TMS): δ = 8.79 (d, $^3J_{\text{H,H}} = 4.68$ Hz, 4 H, H-pyrrole), 8.74 (d, $^3J_{\text{H,H}} = 4.28$ Hz, 4 H, H-pyrrole), 8.22 (d, $^3J_{\text{H,H}} = 7.68$ Hz, 4 H, Ar-H), 8.19 (d, $^4J_{\text{H,H}} = 2.12$ Hz, 4 H, Ar-H), 8.16 (s, 8 H, H-carbazole), 8.06 (s, 2 H), 7.80 (s, 2 H), 7.60 (d, $^3J_{\text{H,H}} = 7.28$ Hz, 4 H, Ar-H), 7.55 (d, $^3J_{\text{H,H}} = 8.52$ Hz, 8 H, H-carbazole), 7.50 (dd, $^4J_{\text{H,H}} = 1.28$, $^4J_{\text{H,H}} = 0.84$, $^3J_{\text{H,H}} = 8.74$ Hz, 8 H, H-carbazole), 7.24 (s, 4 H, H-mesityl), 5.83 (s, 4 H, CH_2), 2.61 (s, 6 H, $2 \times \text{CH}_3$), 1.78 (s, 12 H, $4 \times \text{CH}_3$), 1.47 (s, 72 H, *tert*-butyl) ppm. ^{13}C NMR (100 MHz, CDCl_3 , 25 °C, TMS): δ = 135.08, 132.15, 130.98, 127.71, 126.08, 123.93, 123.72, 122.11, 120.47, 116.40, 109.34 (CH-Ar), 150.04, 149.86, 147.22, 143.56, 143.37, 140.41, 139.18, 138.97, 138.90, 137.50, 133.98, 133.70, 119.54, 119.14 (C-Ar), 54.33 (CH_2), 34.79 (C, *tert*-butyl), 32.03 (CH_3 , *tert*-butyl), 21.62 (CH_3), 21.47 (CH_3) ppm. MALDI-TOF: m/z calcd. for $\text{C}_{148}\text{H}_{146}\text{N}_{14}\text{Zn}$ 2183.114; found 2183.223. Polydispersity index (PDI) = 1.028.

Dendrimer E: Purple solid. ^1H NMR (600 MHz, CDCl_3 , 25 °C, TMS): δ = 8.85 (s, 8 H, H-pyrrole), 8.20 (d, $^4J_{\text{H,H}} = 1.62$ Hz, 8 H, Ar-H), 8.17 (d, $^3J_{\text{H,H}} = 7.74$ Hz, 8 H, Ar-H), 8.15 (s, 16 H, H-carbazole), 8.08 (s, 4 H), 7.79 (s, 4 H), 7.58 (d, $^3J_{\text{H,H}} = 7.68$ Hz, 8 H, Ar-H), 7.54 (d, $^3J_{\text{H,H}} = 8.22$ Hz, 16 H, H-carbazole), 7.48 (dd, $^4J_{\text{H,H}} = 1.68$, $^4J_{\text{H,H}} = 1.62$, $^3J_{\text{H,H}} = 8.25$ Hz, 16 H, H-carbazole), 5.83 (br s, 8 H, CH_2), 1.44 (s, 144 H, *tert*-butyl) ppm. ^{13}C NMR (150 MHz, CDCl_3 , 25 °C, TMS): δ = 135.04, 132.05, 125.95, 123.87, 123.80, 121.98, 120.61, 116.38, 109.27 (CH-Ar), 150.01, 147.15, 143.34, 143.22, 140.35, 138.86, 133.87, 123.67, 120.24 (C-Ar), 54.18 (CH_2), 34.74 (C, *tert*-butyl), 31.98 (CH_3 , *tert*-butyl) ppm. MALDI-TOF: m/z calcd. for $\text{C}_{240}\text{H}_{240}\text{N}_{24}\text{Zn}$ 3521.880 [M^+], 3493.880 [$\text{M} - 28$]; found 3522.791 [$\text{M} + \text{H}^+$], 3495 [$\text{M} - 28 + 2\text{H}^+$]. Polydispersity index (PDI) = 1.028.

Dendrimer F: Purple solid. ^1H NMR (300 MHz, CDCl_3 , 25 °C, TMS): δ = 8.56 (br s, 8 H, H-pyrrole), 8.12 (s, 48 H, 32 H-carbazole, 16 H-phenyl), 7.90 (br s, 8 H, H-triazole/H-phenyl), 7.74 (br s, 8 H, H-phenyl/H-triazole), 7.47 (d, $^3J_{\text{H,H}} = 8.46$ Hz, 32 H, H-carbazole), 7.40 (d, $^3J_{\text{H,H}} = 8.31$ Hz, 32 H, H-carbazole), 5.79 (br s, 16 H, $8 \times \text{CH}_2$), 2.75 (br s, 12 H, $4 \times \text{CH}_3$), 1.93 (br s, 24 H, $8 \times \text{CH}_3$), 1.39 (s, 288 H, *tert*-butyl) ppm. ^{13}C NMR (100 MHz, CDCl_3 , 25 °C, TMS): δ = 149.82, 146.47, 143.50, 143.38, 141.62, 141.32, 140.37, 138.88, 138.74, 138.60, 138.31, 133.93, 131.55, 129.07, 123.88, 123.70, 122.02, 120.17, 118.87, 116.41, 109.26, 108.95 (C-Ar), 49.75 (CH_2), 34.73 (C, *tert*-butyl), 31.97 (CH_3 , *tert*-butyl), 20.01 (CH_3), 17.00 (CH_3) ppm. MALDI-TOF: m/z calcd. for $\text{C}_{448}\text{H}_{476}\text{N}_{44}\text{Zn}$ 6542.28 [M^+], 6514.28 [$\text{M} - 28$]; found 6542.23 [M^+], 6513.37 [$\text{M} - \text{H}^+ - 28$]. Polydispersity index (PDI) = 1.030.

Supporting Information (see footnote on the first page of this article): Experimental procedures, NMR, FTIR, mass spectra of new compounds, gel permeation chromatography (GPC) of porphyrins, absorption and luminescence spectra of porphyrins.

Acknowledgments

This work was supported by a FP-7 grant from the EC for Research, Technological Development and Demonstration Activities

(Dendrimers for Photonic Devices, IRSES-PEOPLE-2009-247260-DphotoD), within the International Research Staff Exchange Scheme. W. D. and J. H. also thank the Fund for Scientific Research – Flanders (FWO), the KU Leuven, and the Ministerie voor Wetenschapsbeleid for continuing financial support. N. T. N. thanks the Ministry of Education and Training, Vietnam International Education Development (VIED) for financial support during his Ph. D in KU Leuven, Belgium.

- [1] J. H. Chou, H. S. Nalwa, M. E. Kosal, N. A. Rakow, K. S. Suslick, in: *The Porphyrin Handbook* (Eds.: K. M. Kadish, K. M. Smith, R. Guilard), Academic Press, San Diego, **2000**, vol. 6, p. 41–121.
- [2] T. Aida, S. Inoue, K. S. Suslick, in: *The Porphyrin Handbook* (Eds.: K. M. Kadish, K. M. Smith, R. Guilard), Academic Press, San Diego, **2000**, vol. 6, p. 133–153.
- [3] T. Malinski, in: *The Porphyrin Handbook* (Eds.: K. M. Kadish, K. M. Smith, R. Guilard), Academic Press, San Diego, **2000**, vol. 6, p. 240–250.
- [4] R. K. Pandey, G. Zheng, in: *The Porphyrin Handbook* (Eds.: K. M. Kadish, K. M. Smith, R. Guilard), Academic Press, San Diego, **2000**, vol. 6, p. 157–224.
- [5] a) M. G. Walter, A. B. Rudine, C. C. Wamser, *J. Porphyrins Phthalocyanines* **2010**, *14*, 759–792; b) B. Walker, C. Kim, T.-Q. Ngyuen, *Chem. Mater.* **2011**, *23*, 470–482; c) A. Yella, H.-W. Lee, H. Nok Tsao, C. Yi, A. Kumar Chandiran, Md. Kh. Nazeeruddin, E. Wei-Guang Diao, C.-Y. Yeh, S. M. Zakeeruddin, M. Grätzel, *Science* **2011**, *334*, 629–634.
- [6] a) A. W. Bosman, H. M. Janssen, E. W. Meijer, *Chem. Rev.* **1999**, *99*, 1665–1674; b) S. Hecht, J. M. J. Frechet, *Angew. Chem.* **2001**, *113*, 76; *Angew. Chem. Int. Ed.* **2001**, *40*, 74–91; c) C. B. Gorman, J. C. Smith, *Acc. Chem. Res.* **2001**, *34*, 60–71; d) D.-L. Jiang, T. Aida, *J. Am. Chem. Soc.* **1998**, *120*, 10895–10901.
- [7] W. Maes, W. Dehaen, *Eur. J. Org. Chem.* **2009**, 4719–4752.
- [8] a) F. Loiseau, S. Campagna, A. Hameurlaine, W. Dehaen, *J. Am. Chem. Soc.* **2005**, *127*, 11352–11363; b) T. H. Xu, R. Lu, X. P. Qiu, X. L. Liu, P. C. Xue, C. H. Tan, C. Y. Bao, Y. Y. Zhao, *Eur. J. Org. Chem.* **2006**, *17*, 4014–4020; c) Y. Li, A. Rizzo, M. Salerno, M. Mazzeo, *Appl. Phys. Lett.* **2006**, *89*, 061125–061125; d) T. Xu, R. Lu, X. Liu, X. Zheng, X. Qiu, Y. Zhao, *Org. Lett.* **2007**, *9*, 797–800; e) K. Albrecht, Y. Kasai, A. Kimoto, K. Yamamoto, *Macromolecules* **2008**, *41*, 3793–3800; f) K. Albrecht, Y. Kasai, Y. Kuramoto, K. Yamamoto, *Chem. Commun.* **2013**, *49*, 6861–6863; g) K. Albrecht, Y. Kasai, Y. Kuramoto, K. Yamamoto, *Chem. Commun.* **2013**, *49*, 865–867.
- [9] A. V. Dijken, K. Brunner, H. Borner, B. M. W. Langeveld, in: *High Efficient OLEDs with Phosphorescent Materials* (Eds.: H. Yersin), Wiley-VCH, Weinheim, Germany, **2008**, p. 326–322.
- [10] a) J. Zhang, X. Wan, X. Xue, Y. Li, A. Yu, Y. Chen, *Eur. J. Org. Chem.* **2010**, 1681–1687; b) R. M. Adhikari, L. Duan, L. Hou, Y. Qiu, D. C. Neckers, B. K. Shah, *Chem. Mater.* **2009**, *21*, 4638–4644.
- [11] a) G. Bubniene, T. Malinauskas, M. Daskeviciene, V. Jankauska, V. Getautis, *Tetrahedron* **2010**, *66*, 3199–3206; b) W. Jiang, L. Duan, J. Qiao, D. Zhang, G. Dong, L. Wang, Y. Qiu, *J. Mater. Chem.* **2010**, *20*, 6131–6137; c) W. Y. Hung, G. M. Tu, S. W. Chen, Y. Chi, *J. Mater. Chem.* **2012**, *22*, 5410–5418; d) M. A. Reddy, A. Thomas, G. Malleshham, B. Sridhar, V. J. Rao, *Tetrahedron Lett.* **2011**, *52*, 6942–6947.
- [12] a) V. V. Rostovtsev, L. G. Green, V. V. Fokin, K. B. Sharpless, *Angew. Chem.* **2002**, *114*, 2708; *Angew. Chem. Int. Ed.* **2002**, *41*, 2596–2599; b) M. Meldal, C. W. Tornoe, *Chem. Rev.* **2008**, *108*, 2952–3015.
- [13] a) A. Eggenspiller, A. Takai, M. E. El-Khouly, K. Ohkubo, C. P. Gros, C. Bernhard, C. Goze, F. Denat, J. M. Barbe, S. Fukuzumi, *J. Phys. Chem. A* **2012**, *116*, 3889–3898; b) G. de Miguel, M. Wielopolski, D. I. Schuster, M. A. Fazio, O. P. Lee, C. K. Haley, A. L. Ortiz, L. Echegoyen, T. Clark, D. M. Guldi, *J. Am. Chem. Soc.* **2011**, *133*, 13036–13054; c) A. Takai, C. P. Gros, J. M. Barbe, R. Guilard, S. Fukuzumi, *Chem. Eur. J.* **2009**, *13*, 3110–3122.
- [14] a) Y. Hizume, K. Tashiro, R. Charvet, Y. Yamamoto, A. Saeki, S. Seki, T. Aida, *J. Am. Chem. Soc.* **2010**, *132*, 6628–6629; b) M. A. Fazio, O. P. Lee, D. I. Schuster, *Org. Lett.* **2008**, *10*, 4979–4982; c) J. D. Megiatto Jr., D. I. Schuster, S. Abwandner, G. de Miguel, D. M. Guldi, *J. Am. Chem. Soc.* **2010**, *132*, 3847–3861.
- [15] a) A. Takai, M. Chkounda, A. Eggenspiller, C. P. Gros, M. Lachkar, J. M. Barbe, S. Fukuzumi, *J. Am. Chem. Soc.* **2010**, *132*, 4477–4489; b) L. L. Pleux, Y. Pellegrin, E. Blart, F. Odobel, A. Harriman, *J. Phys. Chem. A* **2011**, *115*, 5069–5080; c) M. Severac, L. L. Pleux, A. Scarpaci, E. Blart, F. Odobel, *Tetrahedron Lett.* **2007**, *48*, 6518–6522; d) F. Bregier, S. M. Aly, C. P. Gros, J.-M. Barbe, Y. Rousselin, P. D. Harvey, *Chem. Eur. J.* **2011**, *17*, 14643–14662.
- [16] a) N. T. Nguyen, G. Mamardashvili, M. Gruzdev, N. Mamardashvili, W. Dehaen, *Supramol. Chem.* **2013**, *25*, 180–188; b) C. Maeda, S. Yamaguchi, C. Ikeda, H. Shinokubo, A. Osuka, *Org. Lett.* **2008**, *10*, 549–552; c) C. Maeda, P. Kim, S. Cho, J. K. Park, J. M. Lim, D. Kim, J. V.-Weis, M. R. Wasielewski, H. Shinokubo, A. Osuka, *Chem. Eur. J.* **2010**, *16*, 5052–5061.
- [17] J. Zhang, Y. Li, W. Yang, S.-W. Lai, C. Zhou, H. Liu, C.-M. Che, Y. Li, *Chem. Commun.* **2012**, *48*, 3602–3604.
- [18] A. P. Yakubov, M. V. Tsyganov, L. I. Belen'kii, M. M. Krayushkin, *Tetrahedron* **1993**, *49*, 3397–3404.
- [19] A. W. van der Made, R. H. van der Made, *J. Org. Chem.* **1993**, *58*, 1262–1263.
- [20] T. Rohand, E. Dolusic, T. H. Ngo, W. Maes, W. Dehaen, *ARKIVOC* **2007**, 307–324.
- [21] J.-M. Barbe, G. Canard, S. Brandes, R. Guilard, *Eur. J. Org. Chem.* **2005**, *21*, 4601–4611.
- [22] J. S. Lindsey, R. W. Wagner, *J. Org. Chem.* **1989**, *54*, 828–836.
- [23] a) E. Sperotto, G. P. M. van Klink, G. van Koten, J. G. de Vries, *Dalton Trans.* **2010**, *39*, 10338–10351; b) H. B. Goodbrand, N.-X. Hu, *J. Org. Chem.* **1999**, *64*, 670–674.
- [24] A. Hameurlaine, W. Dehaen, *Tetrahedron Lett.* **2003**, *44*, 957–959.
- [25] a) J. E. Hein, V. V. Fokin, *Chem. Soc. Rev.* **2010**, *34*, 1302–1315; b) V. D. Bock, H. Hiemstra, J. H. van Maarseveen, *Eur. J. Org. Chem.* **2006**, 51–68.
- [26] Z. Zhu, J. S. More, *J. Org. Chem.* **2000**, *65*, 116–123.
- [27] M. E. El-Khouly, J. B. Ryu, K. Kay, O. Ito, S. Fukuzumi, *J. Phys. Chem. C* **2009**, *113*, 15444–15453.
- [28] W. Maes, J. Vanderhaeghen, S. Smeets, C. V. Asokan, L. M. V. Renterghem, F. E. Du Prez, M. Smet, W. Dehaen, *J. Org. Chem.* **2006**, *71*, 2987–2994.
- [29] a) M. O. Senge, *J. Photochem. Photobiol. B: Biology* **1992**, *16*, 3–36; b) J. A. Shelnut, X. Z. Song, J. G. Ma, S. L. Jia, W. Jentzen, C. J. Medforth, *Chem. Soc. Rev.* **1998**, *27*, 31–42.
- [30] a) M. Gouterman, *J. Chem. Phys.* **1959**, *30*, 1139–1161; b) M. Gouterman, G. H. Wagniere, L. C. Snyder, *J. Mol. Spectrosc.* **1963**, *11*, 108–127; c) P. J. Spellane, M. Gouterman, A. Antipas, S. Kim, Y. C. Liu, *Inorg. Chem.* **1980**, *19*, 386–391; d) M. Gouterman, in: *The Porphyrins* (Eds.: D. Dolphin), Academic Press, New York, **1978**, vol. 3 p. 1–165.
- [31] a) S. S. Eaton, G. R. Eaton, *J. Am. Chem. Soc.* **1975**, *97*, 3660–3666; b) A. Wolberg, *J. Mol. Struct.* **1974**, *21*, 61–66; c) B. Cheng, O. Q. Munro, H. M. Marques, W. R. Scheidt, *J. Am. Chem. Soc.* **1997**, *119*, 10732–10742; d) D. J. Quimby, F. R. Longo, *J. Am. Chem. Soc.* **1972**, *94*, 5107–5112.
- [32] W. Maes, Th. H. Ngo, G. Rong, A. S. Starukhin, M. M. Kruk, W. Dehaen, *Eur. J. Org. Chem.* **2010**, *13*, 2576–2586.
- [33] a) M. Meot-Ner, A. D. Adler, *J. Am. Chem. Soc.* **1975**, *97*, 5107–5111; b) M. Nappa, J. S. Valentine, *J. Am. Chem. Soc.* **1978**, *100*, 5075–5080.

- [34] a) B. Röder, M. Büchner, I. Rükman, M. O. Senge, *Photochem. Photobiol. Sci.* **2010**, *9*, 1152–1158; b) M. O. Senge, *Chem. Commun.* **2006**, *2*, 243–256.
- [35] V. N. Knyuksho, K. N. Solovyov, G. D. Egorova, *Biospectroscopy* **1998**, *4*, 121–133.
- [36] a) L. Bajema, M. Gouterman, C. B. Rose, *J. Mol. Spectrosc.* **1971**, *39*, 421–431; b) O. Ohno, Y. Kaizu, H. Kobayashi, *J. Chem. Phys.* **1985**, *82*, 1779–1787; c) S. Akimoto, T. Yamazaki, I. Yamazaki, A. Osuka, *Chem. Phys. Lett.* **1999**, *309*, 177–182.
- [37] a) G. G. Gurzadyan, T.-H. Tran-Thi, T. Gustavsson, *J. Chem. Phys.* **1998**, *108*, 385–388; b) J. Aaviksoo, A. Freiberg, S. Savikhin, *Chem. Phys. Lett.* **1984**, *111*, 275–278; c) H. Z. Yu, J. S. Baskin, A. H. Zewail, *J. Phys. Chem. A* **2002**, *106*, 9845–9854.
- [38] Y. Kurabayashi, K. Kikuchi, H. Kokubun, Y. Kaizu, H. Kobayashi, *J. Phys. Chem.* **1984**, *88*, 1308–1310.

Received: August 1, 2013

Published Online: February 11, 2014